THE STABILIZATION MECHANISM OF HIGHLY STABILIZED PARTIALLY PREMIXED FLAMES IN A CONCENTRIC FLOW CONICAL NOZZLE BURNER

Mohy S. Mansour*, A.Elbaz, Mohamed Samy*****
mansour@niles.edu.eg
*Mechanical Power Engineering Department, Faculty of Engineering, Cairo University,
**Mechanical Power Engineering Department, Faculty of Engineering, Helwan University
***National Institute of Laser Enhanced Sciences, Cairo University, Giza, Egypt

Abstract
Many practical combustion systems are based on the mode of partially premixed flames where the interaction between lean and rich pockets improves the flame stability. In our recent work a highly stabilized concentric flow conical nozzle burner has been designed and developed for partially premixed flames. Flow field, temperature and OH radical measurements were conducted outside the cone. The early region of the flame within the cone affects the stability of the flame. So, the aim of the present work is to study the stabilization mechanism inside the cone based on two dimensional measurements of the flow field and temperature field. Five turbulent partially premixed flames have been investigated at Reynolds numbers range between 8.3×10^3 and 14.5×10^3 and equivalence ratio ranges between 2.5 and 4. The turbulent flow field inside and outside the conical quartz nozzle were obtained using a three-dimensional PIV system. The flow filed at the near region inside the cone shows a recirculation zone suggesting air entrainment along the cone wall. This stream of air is likely to be heated by the flame and thus improves the flame stability. Thus, the stabilization mechanism of the conical nozzle burner is mainly affected by the flow pattern inside the cone. This flow field structure improves the stability significantly as compared to similar partially premixed flames without cone. The mean temperature field indicated two distinctive regions at early axial distances, the first of a lower central flame temperature and a second region of a higher flame temperature, which located at a shifted radial distances. These two regions are associated with four distinctive regions of temperature fluctuations. The jet equivalence ratio has a limited effect on flow fields and has relatively milder effect on the temperature field.

1-Introduction
In our newly developed concentric flow conical nozzle (CFCN) burner for highly stabilized partially premixed flames [14], the flames are stabilized using a conical nozzle with a mechanism that controls the degree of partial premixing of the jet. The stability characteristics of the flames show that partial premixed flames are more stable than premixed and non-premixed flames, Mansour, [1]; Mansour et al.,[2]. Similar trend was also observed in high turbulent flames with recirculation zone similar to the primary zone of gas turbine combustor [15, 16]. This is explained by the existence of lean and rich pockets where the reaction takes place within a triple flame environment that provides enough energy source and radicals to sustain the reaction and keep the flame stable. The cone angle in the CFCN burner affects the flame stability as discussed in [13]. The relatively simple geometry of the burner allows the application of theoretical models [14] for fundamental research study in more applied environment than traditional nozzle jet burners.

Burner stability and reduction of pollution levels are the main concerns of designers of industrial burners and many practical combustion systems. Stabilization of flames in either

practical or fundamental flames is the basic and primary subject of interest for most research groups for hundreds of years. The literature includes hundreds of very old research works in this field with several techniques applied at the nozzle exit to stabilize the flames. Examples of those techniques are the swirl flow of Masri and Al-Abadi [3]; Schefer et al. [4]; Ji and Gore [5] and Kalt et al. [6], the pilot flame of Starner and Bilger [7]; Masri et al. [8];Chen et al. [9] and Barlow and Frank [10], and flame holder of Esquiva-Dano et al. [11] and Masri et al. [12]. Partially premixed flames are likely to be more stable than premixed and non-premixed flames, as discussed above, and thus can be more attractive for practical applications, Mansour [1,13].

The CFCN burner has been developed to include both aerodynamic and mixing effects [14]. The burner details are listed below where the degree of partial premixing is controlled within a mixing tube and the aerodynamic is controlled using a cone mounted on the top of the nozzle. This burner provides an excellent opportunity to study partially premixed flames since different degrees of partially premixed can be conveniently generated in the mixing tube ranging from perfectly premixed to non-premixed conditions. Previous experimental studies on this conical flame using sampling techniques have shown that the flame is rather sensitive to the level of partial premixing and nozzle cone angle. An optimal level of partial premixing has been found in which the flame is more stable. Tracer smoke images revealed that a reversal flow exists near the exit of the cone and this was expected to be responsible for the stabilization of this conical flame [13]. However, precise information about the flow and flame structures in the cone was not available due to the limitation of optical access in the metal cone experiments in [1,13]. Understanding the stabilization mechanism of the flames in the CFCN thus requires detailed measurements inside the cone [14].

Accordingly, the main objective of this study is to investigate the flow field at the early region of turbulent of the conical stabilized partially premixed flames using Planar Imaging Velocimeter (PIV) technique. In addition, temperature measurements using fine thermocouple were conduced to provide mean temperature field in several flames to study the mean flame structure within the cone.

2-Experimental Techniques

The aim of the present study is to investigate the flame stability and the detailed structure of partially premixed turbulent flames. The flames in the present work are stabilized on a conical burner nozzle. The measurements are classified into the instantaneous flow field for turbulence and temperature fields for reaction zone analyses. The temperature measurements were conducted using a thermocouple made of platinum/ platinum 13% Rhodium wires of 25 μm diameter. The signal of the thermocouple is digitized using an AD Lab Card (model NI PCI-6020, 16-bit, maximum sampling rate 200 KHz) and is connected to a Compaq computer. At least 50,000 readings are found to be adequate to yield the mean value and temperature fluctuations.

The flow field is measured using three-dimensional Planar Imaging Velocimetry (PIV) technique. However, the current data are used for 2-D only where no swirl is expected and the flow field can be well described in two-dimensional. The current system is three dimensional PIV Dantec model with two CCD cameras and double pulse, two head Nd: YAG laser with pulse energy of 50 mJ at the second harmonic 532 nm. The cameras are HiSense Mkll PIV CCD cameras (model C8484-5205CP) with 1280 x 1024 CCD light sensitive array and equal number of storage cells. The objectives of the cameras are covered with interference filters at 532 nm with a bandwidth of 10 nm. The laser pulse duration is 6 ns and the inter-pulse delay between the two laser heads is controlled according to the flow velocity with a minimum of 0.2 μs for supersonic flow. The cameras and laser are controlled via a control unit connected to PC computer. The images are analyzed using Dantec software where both autocorrelation

and cross-correlation techniques can be applied. Each camera collects two images from the two laser pulses where the images are recorded separately. The laser sheet is created by sheet forming optics that produces expanding laser sheet.

The seeding particles are introduced using a special fluidized bed seeder. The particles used are Titanium dioxide with a diameter of 3 μm in order to follow the flow. The system seeder was tuned to best capture the seeding particles in the reaction zone, where the seeding density was at least 5 particles per interrogation area for cross-correlation. Two mass flow controllers (Alicat Scientific mass and volumetric precision gas flow controller USA) are used to control the air and fuel flow rates. The seeding concentration is adjusted by controlling the amount of air flow through the seeder.

3-Burner

The present burner is similar to the conical burner developed by Mansour [1,13, and 14] with modification of the cone by using quartz glass conical nozzle to enable optical access, in the case of PIV measurements. A schematic illustration of the burner and a photo of the flame and the cone are shown in Fig.(1). The burner consists of two stainless steel tubes where the inner tube supplies air and the outer tube supplies fuel. The exit of the inner tube with air supply is lower than the outer tube by a distance L. Mixing between the two streams of the fuel and air starts at the exit of the inner tube and continues downstream through the mixing distance *L*. The experimental data of El-Mahallawy et al [13] have shown that, at *L/D*=5 (D is the inner diameter of the outer tube), the best flame stability is obtained, i.e., the overall jet equivalence ratio of the fuel/air mixture is minimum to allow a stable combustion. In the present investigation, *L/D*= 5 burner configuration is used, where the burner diameter *D* is 9.7 mm; the half-cone angle is 26^{o}; the height of the cone is 70 mm, and the diameter of the cone exit is 73 mm.

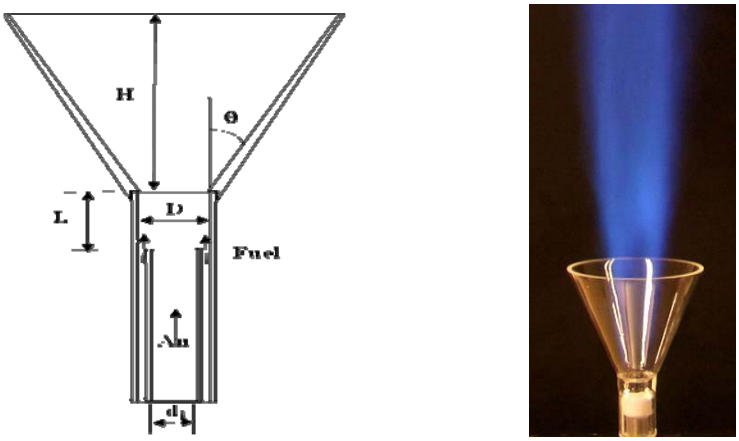

Figure 1. A schematic Diagram of the concentric flow conical nozzle burner and a photo of the flame. The cone angle θ is 26^{o} while the height H is 70 mm.

4-Results and discussions

4.1. Stability limits and selected flames

The stability point, below which the flame is not stable, was obtained by decreasing the fuel flow rate while the air flow rate was kept constant. The stability limit was recorded at the minimum fuel flow rate that corresponds to extinguished flame. The stability limit is obtained for the case of L/D=5, and half cone angle of 26^{o}, where the relation between the jet velocity and jet equivalence ratio at blow- off is illustrated in Fig. (2). Based on the above stability characteristics of the burner, five partially premixed turbulent natural gas (95 % methane, by

volume) flames have been selected in this work. The main parameters of these flames are listed in Table 1, and their positions relative to the stability curve are shown in Fig.(2).

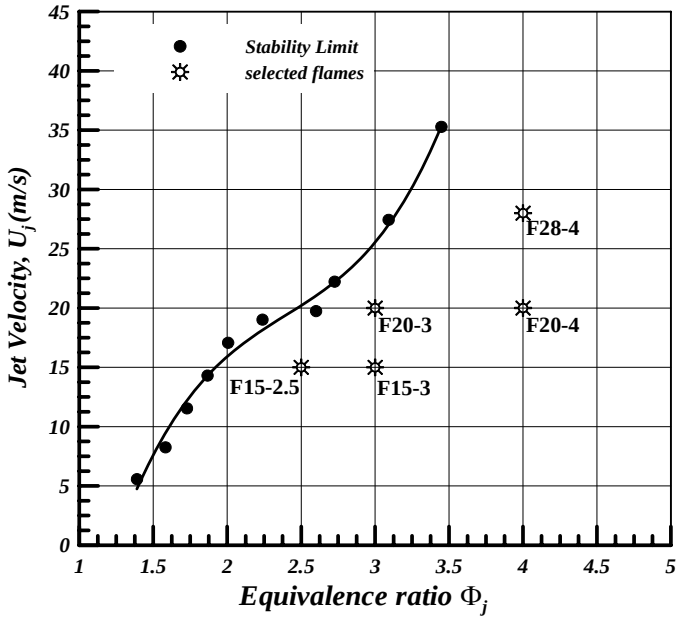

Figure 2. Stability curve of a Natural gas partially premixed flame and the selected flames

Table 1. The main parameters of the investigated flames

Flame	U_j (m/s)	Φ_j	Re
F15-2.5	15	2.5	8363
F15-3	15	3	8214
F20-3	20	3	10952
F20-4	20	4	10598
F28-4	28	4	14838

4.2. Stabilization mechanism

The present burner provides quite highly stable flames at high Reynolds number. The stabilization mechanism has been investigated and discussed based on the instantaneous flow filed measurements inside the cone at the early stage of the flame. Figure (3) shows single shot in flames F15-2.5 and F15-3. In those shots a recirculation zone can be detected near the nozzle exit. This is likely due to the air entrainment along the cone wall. El-Mahalawy et.al [13] have detected air entrainment at the exit of the cone using smoke as a tracer. This suggests that the air is entrained along the wall of the cone. During this pass the air is heated by the flame and this leads to hot air entrainment at the early stage of the flame. This explains the high stability characteristics of the conical flame burner. The recirculation zone at the nozzle exit and air entrainment is very much affected by the cone angle. Thus the stability limit varies with the cone angle as presented by El-Mahalawy et. al [13]. On the other hand normal jet flame without cone has much lower stability limit and this supports our hypothesis and observations. The signal from the PIV system of this recirculation zone is weaker than the main flow because of the lack of seeding particles in the entrained air streams.

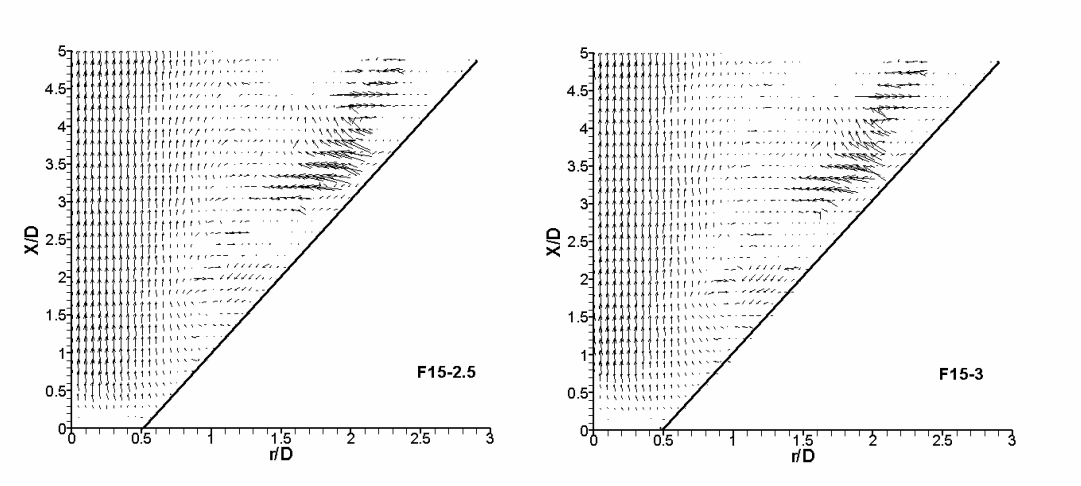

Figure 3. Single shots of the velocity vectors of flames F15-2.5 and F15-3

4.3 The Flow field

The radial velocity profiles of the mean velocity at various axial locations for flame F20-3 are illustrated in Fig.(4). At X/D=2 the velocity profile reveals the presence of a central peak velocity immediately downstream of the exit plane pertinent to the flame jet. However, downstream of X/D=2, Fig.(4) shows steady reduction in the peak velocity of the flame jet but at a different rates. The profiles also indicate the presence of a shear layers associated with the velocity gradients at the flame boundaries at the early region (X/D=2 to 4) inside the cone. By X/D =10 a nearly flat top profile is obtained suggesting the developing stage of the jet flame. The above observations are also evident from the contours of the axial velocity, plotted in Fig.(5). The contours also show a fast attenuation in the peak velocities at the early region of the flame between X/D=2 to X/D=6, further downstream the contours shows a steady attenuation in the peak velocity. This suggests that at the early region the rate of the air entrained from the surrounding is decreased with increasing the axial distance, and this is due to the higher shear stress associated with the early steeper velocity gradient.

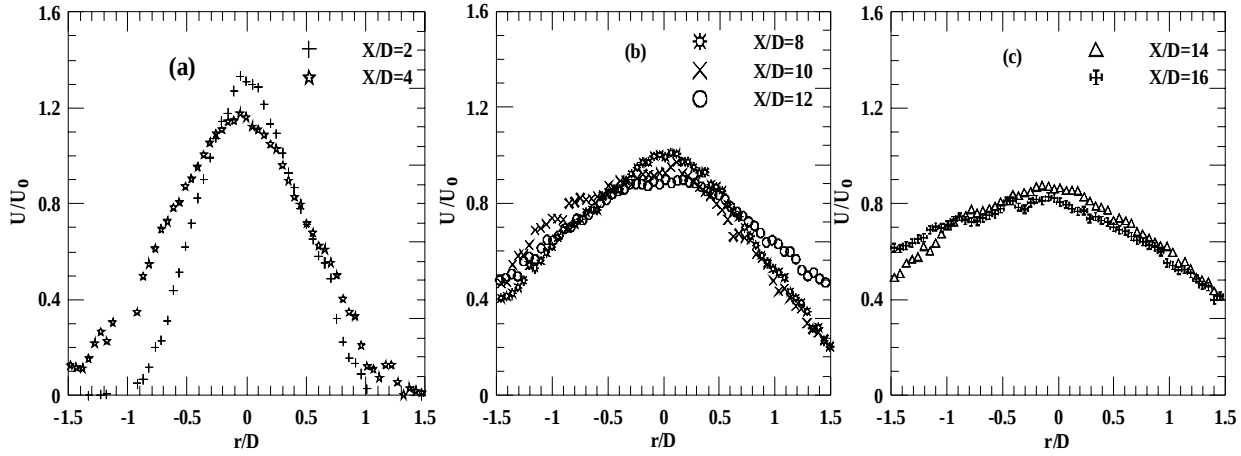

Figure 4. Radial profiles of the mean axial velocity at different axial locations for flame F20-3 [normalized by the bulk flow velocity at the exit of the mixing chamber (20 m/s)]

The profiles of the turbulence intensity ú/U_o are illustrated in Fig.(6) for flame F20-3. The turbulence intensity is relatively high at the early positions near the nozzle exit, between 20 and 30 %. This is higher than the turbulence levels in normal jet flow by about 10 %. This is attributed to the conical nozzle which is likely diverting the flow and creates high turbulence within the cone. In addition, the radial profiles of the turbulence intensity show no

much variation within the core of the jet. This characterizes the conical nozzle flow field as compared to jet flow without cone.

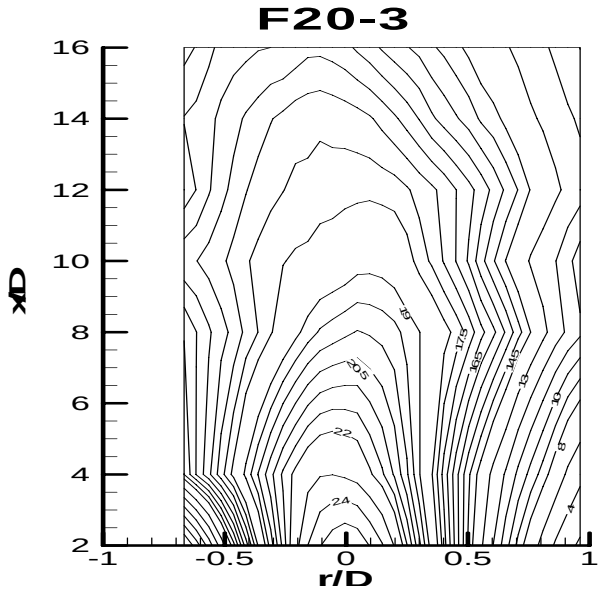

Figure 5. Mean velocity contours for flame F20-3

Close inspection of the profile in Fig.(6-a) shows that two distinctive regions can be identified, with reference to the respective mean velocity profile of Fig.(6-a) at X/D=2, 4. The first region feature rapid rise of the turbulence intensity corresponding to the higher velocity gradient of the outer shear layer of the flame lying between nearly r/D= 0.3 and 0.8. This is followed, towards the flame centerline, by a region of a relatively low nearly constant turbulence intensity covering the flame centerline. The same regions can still be identified in Fig.(6-b) at X/D=8, but with generally higher turbulence intensity levels particularly within the shear layer of the flame.

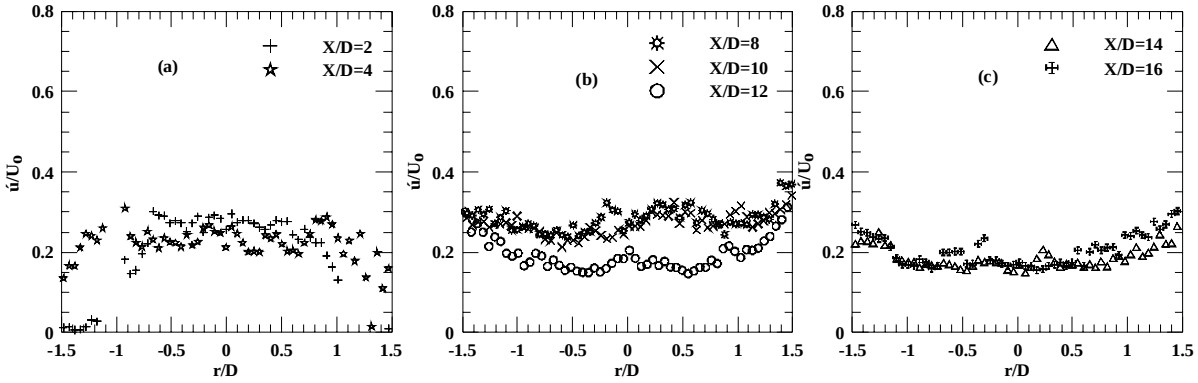

Figure 6. Radial profiles of turbulence intensity at different axial locations for flame F20-3

Moreover, the centre-line turbulence intensity is seen to increase steadily between X/D=8 and 10, this suggests an increase in the production of the turbulence kinetic energy and/or drop in its dissipation rate. Further downstream between X/D=12 to 16, the progresses of the steep gradients featured in the mean velocity profiles and which is responsible for the generation of turbulence kinetics energy, tends to become milder. Consequently, the turbulence intensities drop as the dissipation of the turbulence becomes predominant. This is seen to take place in Fig.(6-c) where the peaks diminish gradually with an associated generally drop in the intensity levels. At X/D=16 the mean velocity distribution features a

flat-top profile with nearly zero velocity gradient at the centerline and an outer shear layer with moderate velocity gradient. This is reflected in Fig.(6-c) in the very low turbulence intensity at the centerline and the modest intensity level across the shear layer. The radial profiles of the axial velocity and turbulence intensity for flames F15-3 and F20-4 are shown in Figs.(7) and (8), respectively. Both sets of profiles show qualitative similarities with those previously examined for Flame F20-3.

Moreover, increasing the equivalence ratio results in faster peak velocity attenuation between the profiles inside the cone and the profiles outside the cone, see Figs. (5) and (8) of flames F20-3, and F20-4, respectively. This is due to the higher air velocity associated with the lower equivalence ratio at the same jet velocity. This indicates that the equivalence ratio has a limited effect on the turbulence intensity level. The effect of the jet velocity at the same equivalence ratio can be seen from Figs.(5) and (7), where the mean velocity profiles show qualitative similarities between F20-3 and F15-3, on the other hand the turbulence intensity profiles provide a lower turbulence intensity inside the cone of F20-3 than F15-3. This is attributed to the higher spread rate of the flame with the higher jet velocity which in turn reduces the boundary layer thickness. This postpones the entrained air to a further downstream distance and hence the lower the turbulence intensity with the higher jet velocity.

The mean axial velocity along the axis is shown in Fig.(9). The axial velocity is decreases along the burner axis, due to the expansion of the cone and hence the deceleration of the flow. As shown up to the axial distance of X/D =5 inside the cone the centerline velocity is decreased in a faster rate than rate of decreased outside the cone.

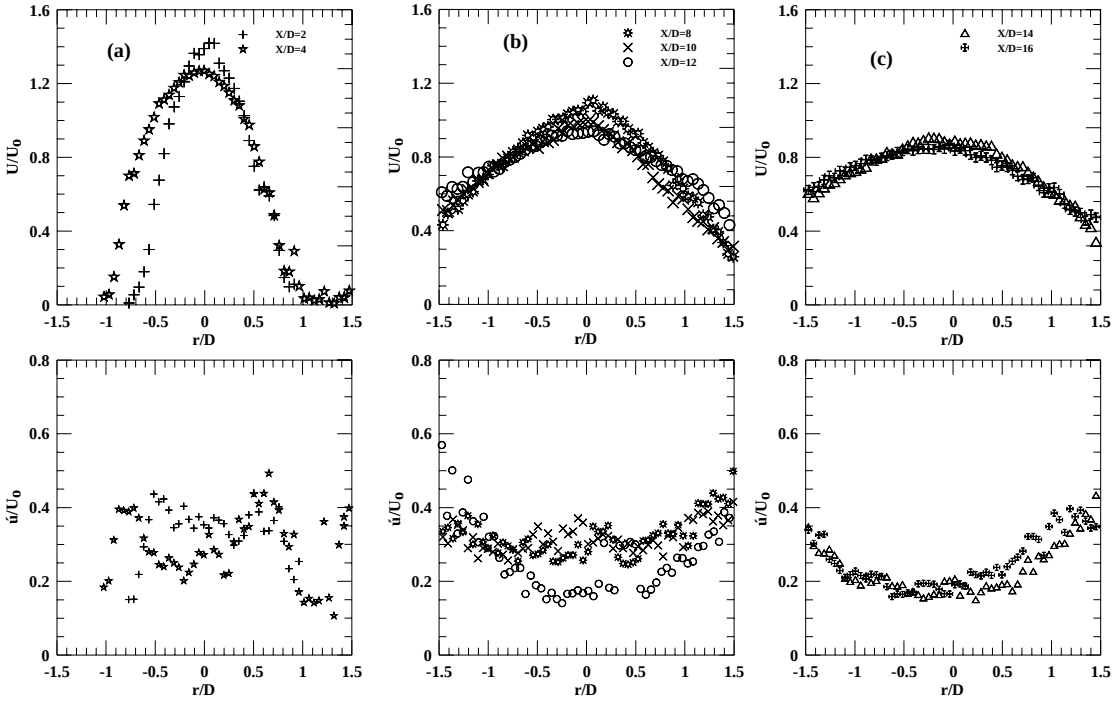

Figure 7. Radial profiles of the mean axial velocity and turbulence intensity at different axial locations for flame F15-3

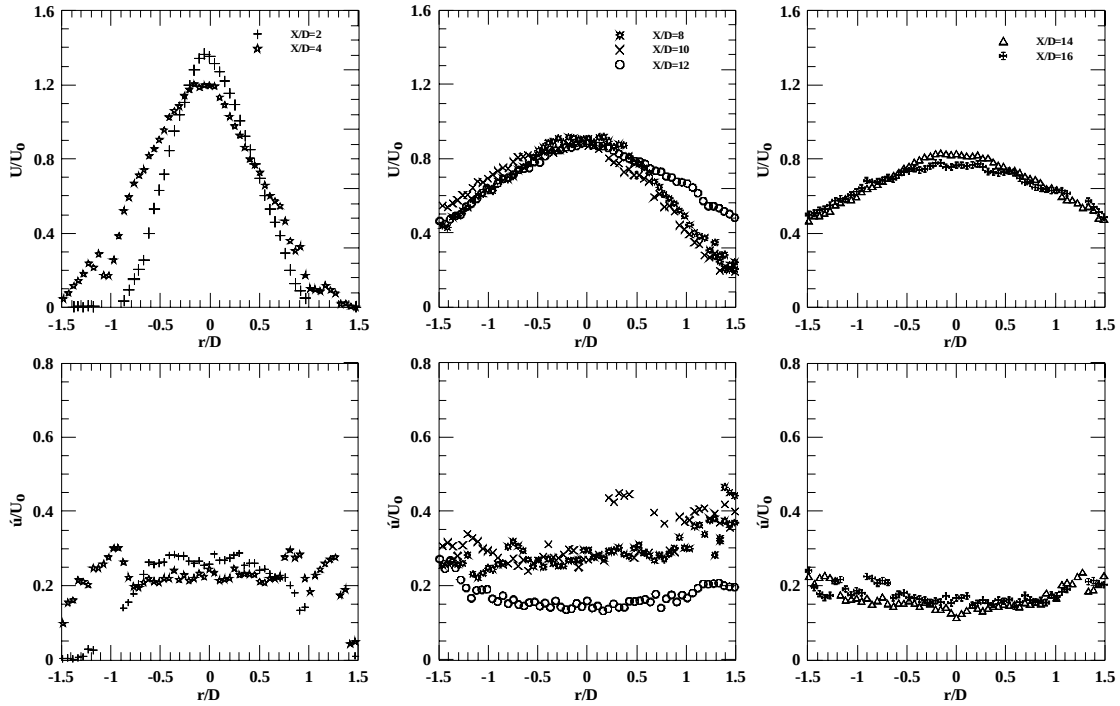

Figure 8. Radial profiles of the mean axial velocity and turbulence intensity at different axial locations for flame F20-4

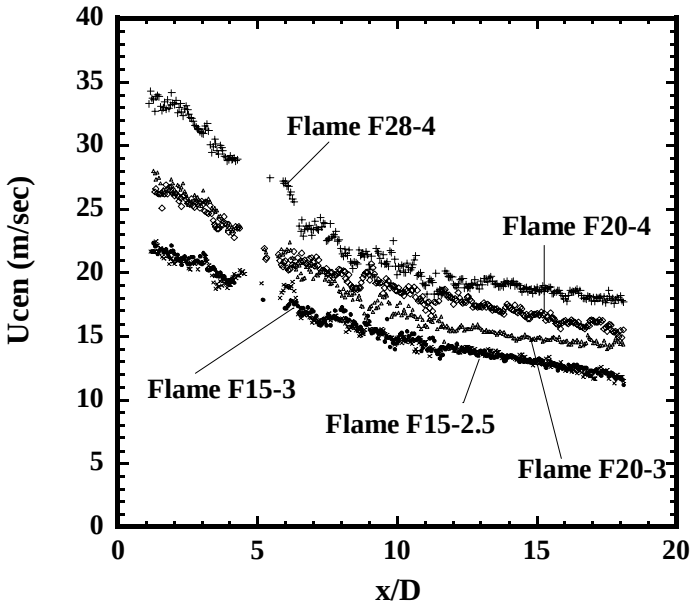

Figure 9. The mean axial centerline velocity

4-4 The temperature field

The radial distribution of mean gas temperature and temperature fluctuation at various axial locations for flame F15-2.5 are illustrated in Fig.(10). The temperature distribution close to the burner exist (at x/D=1) shows almost uniform and relatively low temperature distribution, indicating that the reaction of fuel and air doesn't happen yet. Further downstream axial locations, (1< x/D <8), the mean gas temperature distribution shows a relatively low central region temperature; this is due to the higher strain rate at the flame center line, as well as, the effect of the partially premixed between the fuel and air stream, where the central jet is

containing air. Consequently, the mixing partially premixed between the fuel and air occurs inside the outer burner pipe at air jet shear layer. The low temperature of the central region is increased gradually with increasing the axial distances.

The peak flame temperature occurs at a radial locations shifted away from the flame centerline, indicating that the reaction zone is laying within the layer which have this steeper temperature increase from a relatively low inner temperature region to the point of the peak temperature. This is the feature of the partially premixed flame; this radial location of the peak temperature is gradually shifted to outward direction for the axial distances $1< x/D <8$. This radial spreading of the location of the peak temperature indicates that the reaction zone moves gradually outward toward the outer shear layer. Further downstream axial location ($8 \leq x/D \leq 20$), Figs.(10-b) and (10-c), the centerline temperature increased gradually and the peak flame temperature is gradually decreases and this is due to the gradually fuel depletion. The radial locations of the flame peak temperature execute gradually shifted toward the flame centerline. At x/D=20, the temperature distribution takes a flat profile across almost the flame diameter is obtained.

The profile of temperature fluctuations are illustrated in Fig.(10-d,e,f) for flame F15-2.5. At early axial distances ($1 \leq x/D<8$), close inspection of the profile in Fig.(10-d), four distinctive regions can be identified, with reference to the respective mean temperature profile. The first region features rapid rise and fall of the temperature fluctuations corresponding to the steep temperature gradient lying between radial locations of r/D=1.2 and 1.75. This is followed, towards the flame centerline by a narrow region of very low nearly constant temperature fluctuation covering the region of the maximum flame temperature. The inner region of the flame, which associated with steep temperature increase, follows and is featured in relatively rapid rise of the temperature fluctuation. The fourth and the last region is the inner flame region corresponding to the central flame region features very low temperature fluctuation and covers the core of the jet flame where the mean temperature is nearly constant.

Further downstream axial distances ($8 \leq x/D \leq 12$) of Fig.(10-e), only the first and the fourth regions can still identified but with generally higher temperature fluctuations levels particularly with the outer shear layer of the steep temperature gradient. This suggests an increase in the production of the terms of the turbulent kinetic energy (this was illustrated in the velocity field profiles) and the passive scalar temperature fluctuation and/or drop in the dissipation rate. Moreover, the higher value of the temperature fluctuation which was corresponding to the steep inner temperature increase at the early axial distance is diminished where the temperature gradient becomes milder and hence a drop in the production terms of the temperature fluctuation. Further downstream at $14 \leq x/D \leq 20$ of Fig.(10-f), the flame progress and the steep gradients featured in the mean temperature profiles and responsible for the generation of temperature fluctuation, tend to become milder. Consequently, the temperature fluctuation drop as the dissipation rate becomes predominant at x/D=17 to 20. This is seen to take place in Fig.(10-f), where the peaks diminished gradually with associated general drop in the temperature fluctuation. At x/D=20, the mean temperature distribution features a flat-top profile with nearly zero temperature gradient at the centerline and an outer shear layer with moderate temperature gradient . This is reflected in the low temperature fluctuation at the central region and the modest temperature fluctuation level across the outer flame boundary.

The above observations regarding the mean and temperature fluctuations of flame F15-2.5 broadly apply, both qualitative and quantitative, to mean and temperature fluctuation of flame F15-3, illustrated in Fig.(11). Nonetheless, the following additional observations

regarding this flame F15-3 are to be made. In flame F15-3 shows a relatively lower rate of centerline temperature increase by comparing with flame 15-2.5 see Figs. (10-a,b,c) and (11-a,b,c). Also, the top flat profile of mean temperature in flame F15-2.5 is obtained at earlier axial distance than flame F15-3. This is due to the higher jet equivalence ratio which delayed the compellation of the combustion of flame F15-3 for further more axial distances.

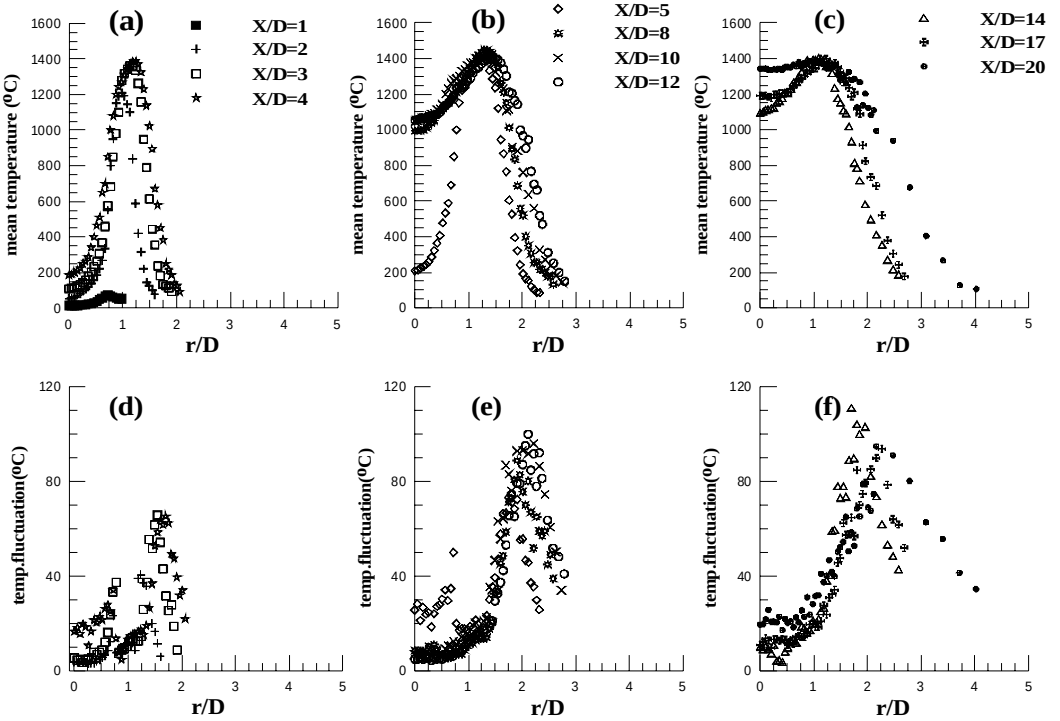

Figure 10. Radial profile of temperature and temperature fluctuation for flame F15-2.5

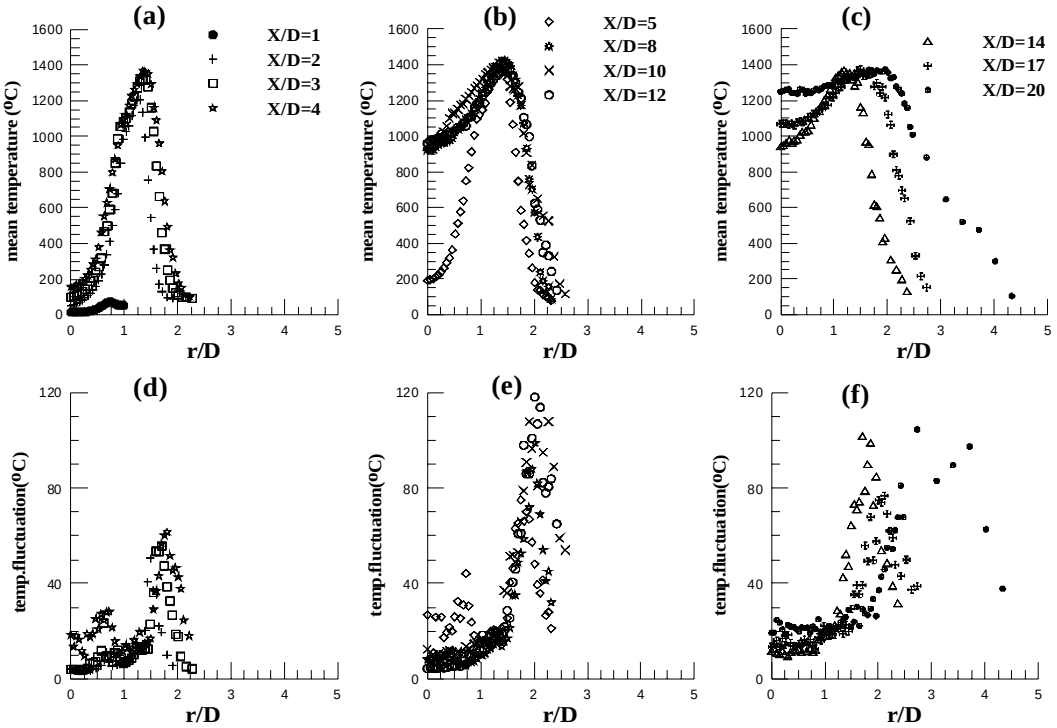

Figure 11. Radial profile of temperature and temperature fluctuation for flame F15-3

Conclusions

The flow field, the temperature field, and stabilization mechanism of a partially premixed natural gas-air flame stabilized on a conical jet burner have been investigated and discussed in the present work using 3D PIV system and fine thermocouple measurements. The flow fields of five flames at different jet velocities and equivalence ratios have been mapped. The flame in the conical nozzle burner was found to be stabilized through the creation of a reversal flow near the inside wall of the cone. This reversed flow heated the entrained air from the surrounding through its passage to the root of the flame. The turbulence field conforms well to the mean velocity field and generation of turbulence kinetic energy which prominent in region of the velocity gradients in the case of the lower jet velocity. Increasing the jet velocity at the same equivalence ratio increases the spread rate inside the cone and the lower the turbulence intensity inside the cone and smaller the thickness of the boundary layer. The jet equivalence ratio has no effect on the flame flow field, while a relatively low effect on the mean temperature field at the early axial distances. The temperature fluctuation fields confirm well with the mean temperature field, where the higher temperature fluctuations are confirmed at the regions of relatively higher temperature gradients.

Acknowledgement

This work was partly sponsored by the Swedish Research Council VR, SSF and STEM through CeCOST and the Swedish International Development Agency (SIDA) fund for the MENA countries through the joint project between Egypt and Sweden.

References

[1] Mansour, M.S. (2000) A concentric flow conical nozzle burner for highly stabilized partially premixed flames. Combust. Sci. Technol., 152, 115–145.

[2] Mansour, M.S., Bilger, R.W., and Dibble, R.W. (1989) Raman/ rayleigh and miescattering measurements in a reverse flow reactor close to extinction. Proc.Combust. Instit., 22, 711–719.

[3] Masri, A.R. and Al-Abdeli, Y.M. (2003) Stability characteristics and flow fields of turbulent non-premixed swirling flames. Combust. Theory Model., 7(4), 731–766.

[4] Schefer, R.W., Wicksall, D.M., and Agrawal, A.K. (2002) Combustion of hydrogen- enriched methane in a lean premixed swirl-stabilized burner. Proc. Combust. Instit., 29, 843–851.

[5] Ji, J. and Gore, J.P. (2002) Flow structure in lean premixed swirling combustion. Proc. Combust. Instit., 29, 861–867.

[6] Kalt, P.A.M., Al-Abdeli, Y.M., Masri, A.R., and Barlow, R.S. (2002) Swirling turbulent non-premixed flames of methane: flow field and compositional structure. Proc. Combust. Instit., 29, 1913–1919.

[7] Starner, S.H. and Bilger, R.W. (1985) Characteristics of a piloted diffusion flame designed for study of combustion turbulence interactions. Combust. Flame, 61, 29–38.

[8] Masri, A.R., Dibble, R.W., and Barlow, R.S. (1996) The structure of turbulent non-premixed flames revealed by raman-rayleigh-lif measurements. prog. Energy Combust. Sci., 22, 307–362.

[9] Chen, Y.-C., Peters, N., Schneemann, G.A., Wruck, N., Renz, U., and Mansour, M.S. (1996) The detailed flame structure of highly stretched turbulent premixed methane-air flames. Combust. Flame, 107, 223–244.

[10] Barlow, R.S. and Frank, J.H. (1998) Effects of turbulence on species mass fractions in methane=air jet flames. Proc. Combust. Instit., 27, 1087–1096.

[11] Esquiva-Dano, I., Nguyen, H.T., and Escudie, D. (2001) Influence of a bluff body's shape on the stabilization regime of non-premixed flames. Combust. Flame, 127, 2167–2180.

[12] Masri, A.R., Dally, B.B., Barlow, R.S., and Carter, C.D. (1994) The Structure of the recirculation zone of a bluff-body combustor. Proc. Combust. Instit., 25, 1301–1308.

[13] El-Mahallawy, F. Abdelhafez, A. and Mansour, M.S. (2007) Mixing and Nozzle Geometry Effects on flame structure and stability. Combust. Sci. Technol., 1179, 249–263.

[14] B. Yan, B. Li, E. Baudoin, C. Liu, Z.W. Sun, Z.S. Li, X.S. Bai, M. Alden, G. Chen, M.S. Mansour. (2010) Structure and stabilization of low calorific value gas turbulent partially premixed flames in a conical burner, Experimental Thermal and Fluid Science., 34, 412-419.
[15] Mansour, M.S., Chen, Y.-C., and Peters, N. (1999) Highly strained rich methane flames stabilized by hot combustion products. Combust. Flame, 116, 136-153.
[16] Masri, A.R., Dally, B.B., Barlow, R.S., and Carter, C.D. (1994) The Structure of the recirculation zone of a bluff-body combustor. Proc. Combust. Instit., 25, 1301–1308.